Experimental Neurology **170,** 36–47 (2001)
doi:10.1006/exnr.2001.7700, available online at http://www.idealibrary.com on IDEAL®

Selective Antibody-Induced Cholinergic Cell and Synapse Loss Produce Sustained Hippocampal and Cortical Hypometabolism with Correlated Cognitive Deficits

Susan E. Browne,* Ling Lin,† Anna Mattsson,† Biljana Georgievska,† and Ole Isacson†,[1]

**Department of Neurology and Neuroscience, Weill Medical College at Cornell University, A502, 525 East 68th Street, New York, New York 10021; and †Neuroregeneration Laboratory, Department of Neurology and Psychiatry, Harvard Medical School, McLean Hospital, 115 Mill Street, Belmont, Massachusetts 02178*

Received October 5, 2000; accepted March 30, 2001

The physiological interrelationships between cognitive impairments, neurotransmitter loss, amyloid processing and energy metabolism changes in AD, cholinergic dementia and Down's syndrome are largely unknown to date. This report contains novel studies into the association between cognitive function and cerebral metabolism after long-term selective CNS cholinergic neuronal and synaptic loss in a rodent model. We measured local cerebral rates of glucose utilization (^{14}C-2-deoxyglucose) throughout the brains of awake rats 4.5 months after bilateral intraventricular injections of a cholinotoxic antibody directed against the low-affinity NGF receptor (p75 NGF) associated with cholinergic neurons (192 IgG-saporin). Permanent cholinergic synapse loss was demonstrated by [^{3}H]-vesamicol *in vitro* autoradiography defining presynaptic vesicular acetylcholine (ACh) transport sites. While other metabolic studies have defined acute and transient glucose use changes after relatively nonspecific lesions of anatomical regions containing cholinergic neurons, our results show sustained reductions in glucose utilization in brain regions impacted by cholinergic synapse loss, including frontal cortical and hippocampal regions, relative to glucose use levels in control rats. In the same animals, impaired cognitive spatial performance in a Morris water maze was correlated with reduced glucose use rates in the cortex and hippocampus at this time point, which is consistent with increased postmortem cortical and hippocampal amyloid precursor protein (APP) levels (45, 46). These results are consistent with the view of cholinergic influence over metabolism, APP processing, and cognition in the cortex and hippocampus.

INTRODUCTION

Alzheimer's disease (AD) is a complex neurological disorder typified by a progressive cognitive decline. The disease is neurochemically and pathologically characterized by APP mismetabolism, extracellular deposition of amyloid β-peptide (Aβ)-containing neuritic plaques and intraneuronal tau-containing fibrillary tangles. There is also extensive synaptic and neuronal loss in allo- and neocortex, along with a marked degeneration and loss of cholinergic neurons within the basal forebrain (BF), and reduced choline acetyl transferase (ChAT) in cortex and hippocampus (7, 8, 10, 14, 66, 79). Another common finding in affected individuals is reduced glucose metabolism in cortical and hippocampal regions, detected by positron emission tomography (PET), notable as these are the primary projection targets of BF cholinergic efferents (19, 22, 23).

The definitive roles and interactions of cognitive, cholinergic, energy dysfunction and amyloid deposition in the pathogenesis of AD are still unclear (4, 5, 28, 81). Experimental studies, both *in vitro* and *in vivo*, indicate that cholinergic function may regulate Aβ formation by modulating APP processing (45, 56). APP cleavage at either the N- or C-terminus of the Aβ domain (by β- or γ-secretase, respectively) generates Aβ which can aggregate to form amyloid plaques. In contrast, cleavage within the Aβ domain by α-secretase results in secretion of soluble peptide (APPs) into the extracellular space, which has been postulated to have neuroprotective or neurotrophic effects (50). *In vitro* and *in vivo* (45, 53, 58) preclinical studies showed that activation of muscarinic acetylcholine (ACh) receptors, primarily muscarinic ACh M1, can accelerate α-secretase processing of APP, potentially reducing neuronal content and extracellular release of putatively harmful Aβ peptides. This reduction of Aβ levels has also recently been demonstrated after M1 agonist treatment in AD patients (57). Removal of the basal forebrain cholinergic

[1] To whom correspondence and reprint requests should be addressed. Fax: (617) 855 3284. E-mail: isacson@helix.mgh.harvard.edu.

0014-4886/01 $35.00

innervation of cortex and hippocampus permanently increases APP expression in deafferented regions and reduces APP secretion into extracellular space (40, 45, 46, 70). The specificity of the cholinergic system for APP regulation within the forebrain is supported by findings that cortical dopaminergic denervation by 6-OHDA lesions in rats had no effect on APP levels (46).

Previous functional studies of the BF cholinergic system have been hampered by the lack of a selective cholinergic neurotoxin (9, 47, 60). In this study we used a monoclonal antibody to the low affinity nerve growth factor (NGF) receptor, 192 IgG, coupled to a ribosome-inactivating cytotoxin, saporin, to lesion the cholinergic BF projection, and examined the functional affects on glucose metabolism and cognition. NGF provides trophic support to cholinergic BF neurons that express high levels of the low affinity NGF receptor p75NGFR in the adult rat brain. Intracerebroventricular (i.c.v.) injection of 192 IgG-saporin selectively destroys p75NGFR-bearing cells, which include principally cholinergic BF neurons and, to a much lesser extent, cerebellar purkinje cells. Therefore, intraventricular injection of 192 IgG-saporin produces an almost complete lesion of cortical and hippocampal cholinergic afferents arising from the BF, while sparing other neuronal populations within the BF and other brain regions (29, 71). We measured local cerebral glucose use by [^{14}C]-2-deoxyglucose autoradiography in conscious rats 4.5 months after lesioning the basal forebrain cholinergic system via i.c.v. injections of 192 IgG-saporin. Cholinergic denervation was verified by assessment of [^{3}H]-vesamicol binding to localize the presynaptic vesicular acetylcholine transporter. Four days prior to the 2-deoxyglucose procedure, animals underwent behavioral testing in a Morris water maze.

MATERIALS AND METHODS

Animals. Sixteen female, adult Sprague–Dawley rats (200–230 g preoperative weights) were used in the experiments (Charles River Laboratories, MA). Rats were held in a controlled temperature environment under a 12-h light/dark cycle, and allowed free access to food and water for the duration of the experimental period. The two groups were 192 IgG-saporin lesioned (n = 8) and aged-matched controls (n = 8) housed in parallel.

Cholinergic lesion surgery. Rats were anaesthetized using ketaset/xylazine (67/6.7 mg/kg i.m., Sigma, St. Louis, MO) and placed in a stereotactic frame (David Kopf, Tujunga, CA). Bilateral i.c.v. injections were made at the following stereotaxic coordinates: AP −0.6 mm (from bregma); L ± 1.5 mm (lateral to midline); V −3.5 mm (below dura); incisor bar set −3.4 mm (45, 64). 192 IgG-saporin (total 5 μg, 1 μg/μl, 2.5 μl/side; 1 μ/min; Chemicon International, Temecula, CA) was injected via a 10 μl Hamilton syringe connected to a 26-gauge needle with a 45° beveled tip. Needles were left in place for 3-min before removal. Animals received daily injections of sterile saline (0.9%; 5 ml s.c.) for 1 week postsurgery to minimize dehydration. All rats appeared normal with no weight loss by two weeks postsurgery.

Behavioral analysis. Eighteen weeks postsurgery, rats received behavioral tests to assess parameters of cognitive performance in a Morris water maze task, as previously described (43, 46) (Poly-Track Video Tracking System, San Diego Instruments, San Diego, CA). Briefly, a circular six-foot tank was filled with water at room temperature and a clear plexiglass platform was submerged one inch underwater in the southwest quadrant of the pool. On the day immediately preceding the test, animals received two 1-min trials in the tank without the platform present to allow for habituation to the maze. Starting on Day 1, the rats were given six trials per day for five consecutive days, each trial lasting a maximum of 60 s or until the rat escaped to the platform. If the rats failed to find the platform, the experimenter placed them there. A 15-s rest period on the platform followed each trial. In each trial the rats were randomly placed in the tank from four fixed points (designated North, South, East and West). On the last day of testing the rats received a "spatial probe trial," where the platform was removed from the tank and the rats were allowed to swim for 60 s. Total swim time (escape latency), distance to the platform and swim speed as well as time spent in the target quadrant were recorded for each rat for each trial.

[^{14}C]-2-Deoxyglucose autoradiography ([^{14}C]-2-DG). Local cerebral rates of glucose use were measured in conscious rats by Sokoloff's [^{14}C]-2-DG procedure, four days after behavioral tests, (75). Briefly, rats (375–425 g) were anesthetized with 1.0% halothane in a 70/30% N_2O/O_2 mix, and PE50 polyethylene cannulae inserted into two femoral arteries and one vein. The incision sites were sutured closed after application of 2% lidocaine gel, and animals were restrained by means of a loosely fitting plaster cast, and allowed to recover from anesthesia for 2 h. The 2-DG procedure was initiated by a bolus injection of 50 μCi [^{14}C]-2-DG i.v. over 30 s in 0.7 ml heparinized saline. Over the subsequent 45 min, 14 timed arterial blood samples were collected for analysis of blood glucose and ^{14}C levels. Blood gases (pCO_2, pO_2) were measured 5 min before and 35 min after isotope administration. After 45 min the rats were decapitated, their brains removed and rapidly frozen in isopentane at −43°C. Brains were cut into 20-μm-thick coronal cryostat sections and mounted onto heated coverslips. Serial sections were collected in triplicate at 200-μm intervals throughout the brain and exposed to ^{14}C-sensitive film (Kodak Biomax MR-1) along with precalibrated ^{14}C standards (Amer-

sham) for 7 days. Local tissue isotope concentrations in areas of interest were then determined from the autoradiograms by computer-assisted densitometry with reference to the ^{14}C standards. Local rates of glucose use were then calculated by application of Sokoloff's operational equation for the procedure (75).

Vesicular ACh transporter: [^{3}H]-Vesamicol binding. Localization of the presynaptic acetylcholine uptake transporter was achieved by densitometric assessment of specific [^{3}H]-vesamicol binding in 20-μm-thick cryostat sections immediately adjacent to those used for glucose use measurement, thaw-mounted onto gelatin-subbed slides. Prior to ligand incubation, residual ^{14}C was eluted from the thawed sections by three successive 1 min washes in buffer (50 mM Tris–HCI, containing 120 mM NaCI, 5 mM KCI, 1 mM $MgCI_2$, 2 mM $CaCI_2$; pH 7.4) (11). Sections were then preincubated in buffer for 20 min (25°C). For total binding, sections were incubated in buffer containing 5 nM [^{3}H]-vesamicol, with 15M 1,3-*di*(2-tolyl)guanidine (DTG) to displace vesamicol binding to opioid receptors (60 min, 25°C). For nonspecific binding, adjacent sections were incubated in identical conditions with the addition of 15 μM unlabeled vesamicol. Sections were then washed twice for 30 s in 50 mM Tris–HCI, once for 10 s in 5 mM Tris–HCI, once for 10 s in deionized water (4°C), and then dried overnight in a stream of air (25°C). Autoradiograms were generated by exposing sections to [^{3}H]-sensitive Hyperfilm (Amersham) along with precalibrated ^{3}H standards in light-tight X-ray cassettes for 4 weeks. Transporter densities in discrete brain regions were then quantified by computer-assisted densitometry (MCID Image Analysis system, Imaging Research Inc., St. Catherine's, ON) by measuring the optical densities of ^{3}H binding in regions of interest. Tissue concentrations were calculated by extrapolation from the optical densities of the precalibrated standards. Specific [^{3}H]-vesamicol binding was then calculated by subtracting the amount of non-specific ^{3}H binding from total ^{3}H binding in a given region.

Data analysis. Glucose use values were measured bilaterally in 24 discrete CNS regions. Regions of interest were chosen to reflect cholinergic nuclei, cholinergic projection targets, and control regions lacking major direct cholinergic innervation. Presynaptic vesicular ACh transporter densities were determined in the same 22 regions in 20-μm-thick brain sections adjacent to the sections used for glucose use measurements. Densitometric data in each brain region examined were compared between lesioned and nonlesioned animals using an unpaired Student's *t* test. Correlational analysis with corrections for multiple comparisons were performed on specific glucose utilization values and behavioral performance (JMP program, Version 3.1.6, SAS Institute). Differences were considered statistically significant when $P < 0.05$.

TABLE 1

Physiological Variables in Basal Forebrain Lesioned Rats

Physiological Variables	Nonlesioned	Saporin-lesioned
Arterial plasma glucose (mg/dl)	160 ± 14	192 ± 27
Rectal temperature (°C)	99.5 ± 0.5	98.7 ± 0.5
*p*O2 (mmHg)	65.7 ± 2.1	63.2 ± 2.8
*p*CO2 (mmHg)	35.7 ± 2.4	33.6 ± 2.4
*p*H	7.5 ± 0.0	7.5 ± 0.0

Note. Data are presented as mean ± SEM, variables measured 5 min before initiation of the [^{14}C]-2-deoxyglucose procedure in 192 IgG-saporin-lesioned ($n = 6$) and nonlesioned (control, $n = 6$) rats. There were no statistically significant differences between saporin-lesioned and nonlesioned (control) animals in any of the parameters measured ($P > 0.05$, Student's unpaired *t* test).

RESULTS

Behavioral Tests

Rats showed behavioral deficits in the Morris water maze test 18 weeks after bilateral i.c.v. injections of 192 IgG-saporin, similar to those previously described (40, 43, 46). Lesioned animals generally exhibited significantly longer escape latencies. On the final day of testing, the performance of non-lesioned animals was 24 ± 3 s vs 9 ± 2 s of lesioned rats ($P < 0.001$). In the spatial probe task trial on day 1, 2, and 5, lesioned animals spent significantly less time in the target quadrant than non-lesioned controls (day 5: 39 ± 3% vs 58 ± 3%, lesioned vs control rats, $P < 0.001$). Swim speed was slightly higher in the lesioned animals on day 1, 2, 3, and 5 of testing (day 5 = 8.69 ± 0.43 vs 7.29 ± 0.23, lesioned vs control rats, $P < 0.05$).

[^{14}C]-2-Deoxyglucose Autoradiography ([^{14}C]-2-DG)

(i) Physiological variables. On the day of the [^{14}C]-2-DG procedure the partially restrained, conscious rats were lively and alert, and exhibited normal grooming and sniffing behavior throughout the experimental period. Physiological variables measured 5 min before commencement of the [^{14}C]-2-DG procedure are presented in Table 1. None of the measured parameters (pCO_2, pO_2, *p*H, arterial plasma glucose concentration and rectal temperature) differed significantly between lesioned and control animals. Measured pO_2 levels in both control and lesioned rats were slightly below normal physiological levels, but all other parameters were within normal physiological limits.

(ii) Local cerebral glucose utilization. The effects of 192 IgG-saporin i.c.v. injections on cerebral glucose use 18 weeks post-lesion are presented in Table 2. Statistically significant ($P < 0.05$) reductions in glucose use were evident in four brain regions after cholinergic deafferentation, while trends toward reduced glucose use were evident in several other regions including

TABLE 2

Local Cerebral Glucose Utilization Chronically after Basal Forebrain Lesions

Region	Nonlesioned	Saporin-lesioned
BF Cholinergic Projection Targets:		
Prefrontal cortex I–III	89 ± 5	77 ± 4
Prefrontal cortex IV	97 ± 6	82 ± 5
Prefrontal cortex V–VI	76 ± 4	64 ± 4
Frontal cortex I–III	89 ± 5	75 ± 5
Frontal cortex IV	98 ± 6	83 ± 5
Frontal cortex V–VI	74 ± 4	63 ± 4
Parietal cortex I–III	88 ± 5	78 ± 6
Parietal cortex IV	96 ± 5	83 ± 6
Parietal cortex V–VI	81 ± 4	64 ± 4*
Hippocampus: CA1 (rostral)	51 ± 2	36 ± 4*
Hippocampus: CA3 (rostral)	59 ± 3	45 ± 5*
Dentate Gyrus mol. (caudal)	73 ± 3	57 ± 5*
Amygdala	47 ± 3	40 ± 3
Cholinergic Regions:		
Nucleus accumbens	76 ± 5	71 ± 3
Rostral septum	67 ± 3	65 ± 3
Striatum: dorsolateral	81 ± 5	72 ± 4
Striatum: dorsomedial	73 ± 6	64 ± 4
Striatum: ventromedial	73 ± 5	66 ± 3
Nucleus basalis magnocellularis	88 ± 6	74 ± 4
Diagonal band of broca (DBB)	70 ± 4	61 ± 3
Medial septum	69 ± 4	61 ± 4
Other regions:		
Globus pallidus	48 ± 3	43 ± 2
Substantia nigra pars reticulata	46 ± 3	40 ± 3
Substantia nigra pars compacta	67 ± 4	60 ± 5
Cerebellum: grey	42 ± 4	39 ± 1
Cerebellum: white	20 ± 2	21 ± 1

Note. Data are mean ± SEM local cerebral rates of glucose utilization (μmol/100 g/min) 18 weeks after bilateral i.c.v. injection of 192 IgG-saporin (saporin-lesioned), and in control (nonlesioned) animals ($n = 6$ per group). Roman numerals indicate layers of cerebral cortex. *$P < 0.05$, significantly reduced glucose utilization relative to control values (Student's unpaired t test).

most notably primary projection targets for NBM/septum cholinergic efferents.

Basal forebrain (BF) cholinergic projection sites. Glucose utilization was significantly reduced in the hippocampus CA1 and CA3 subfields (−32 and −29%, respectively), in the dentate gyrus molecular layer (−22%; Fig. 1) and in the deep layers of parietal cortex (−21%). In addition, trends toward glucose use reductions (−14–21%) were evident in other primary cholinergic projection targets of basal forebrain nuclei, including prefrontal, frontal and parietal cortices, and the amygdaloid nucleus.

Basal forebrain regions. Glucose utilization values did not significantly differ between lesioned and nonlesioned animals in any of the eight basal forebrain regions examined containing cholinergic neuron cell bodies, although trends toward reduced metabolism were evident in the nucleus basalis magnocellularis (NBM), diagonal band of Broca (DBB), and striatal subregions.

Secondary BF projection sites and other areas. Glucose use values were unaltered in globus pallidus, substantia nigra pars compacta and reticulata, and cerebellar regions.

[^{3}H]-Vesamicol Binding

[^{3}H]-Vesamicol binds to and locates vesicular acetylcholine (ACh) uptake sites (69). [^{3}H]-Vesamicol was used in this study to locate and quantify presynaptic cholinergic terminals and therefore to provide an index into the effect of 192 IgG-saporin i.c.v. injections on cholinergic innervation within the brain. Since vesamicol is also shown to have some affinity for binding to opioid receptors (15) we included 1,3-*di*(2-tolyl)guanidine (DTG) in the incubation buffer to displace opioid receptor binding. 192 IgG-saporin injections markedly reduced [^{3}H]-vesamicol binding 18 weeks postlesion in BF projection zones and in some BF regions. [^{3}H]-Vesamicol binding levels throughout the brain are presented in Table 3. Findings confirm that 192 IgG-saporin i.c.v. injections did result in a chronic loss of cholinergic projection terminals.

Basal forebrain (BF) cholinergic projection sites. [^{3}H]-Vesamicol binding densities were markedly reduced in the hippocampus CA1 and CA3 subfields (−71 and −65%, respectively), and in the dentate gyrus molecular layer (−72%) 18 weeks after 192 IgG-saporin lesions, relative to levels in non-lesioned, control animals ($P < 0.05$). In addition, marked trends towards reduced [^{3}H]-vesamicol binding were also evident in pre-frontal cortex sublayers (−50–63%) as demonstrated in Fig. 1, and to a lesser extent in parietal and frontal cortices, although these did not reach statistical significance with the group sizes employed.

Basal forebrain region. [^{3}H]-Vesamicol binding was significantly decreased in the ventromedial striatum 18 weeks postlesion (−60%, $P < 0.05$; Fig. 1), and showed a trend toward reduction in the nucleus accumbens (−31%).

Secondary BF projection sites and other areas. [^{3}H]-Vesamicol binding densities in 192 IgG-saporin lesioned rats did not significantly differ from control levels in any of the other CNS regions examined.

Correlation Analyses: Behavioral Deficits and Cerebral Glucose Metabolism

Although both escape latency and distance swum are usually good indicators of spatial performance impairment in rats with cholinergic deficits, it is possible that swim speed may affect escape latency in the water maze. Therefore, we chose to correlate the spatial probe task performance (percentage of time spent in target-quadrant) measured in individual animals, with their respective local rates of glucose utilization in the 24 different brain regions examined. Results for this

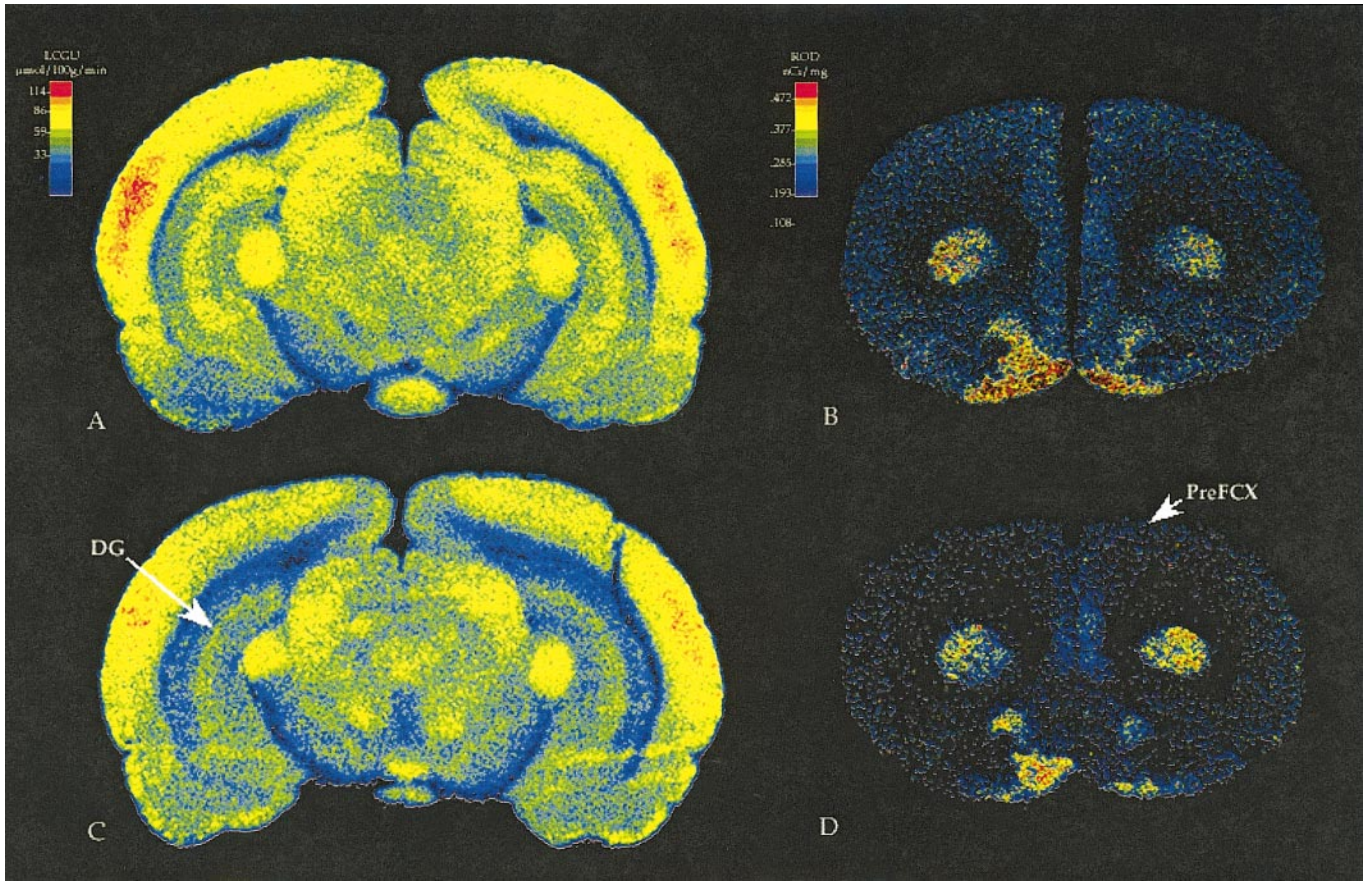

FIG. 1. Loss of cholinergic terminals is associated with reduced glucose use in downstream cholinergic projection zones four months after intraventricular injections of IgG-saporin in rats. Representative sections show local rates of cerebral glucose use (LCGU, μmol/100 g/min) at the level of the medial geniculate nuclei (A, C), and ^{3}H-vesamicol binding levels (nCi/mg tissue) at the level of the prefrontal cortex (B, D). Color-coded images are from 20-μm-thick coronal brain sections from the same IgG-saporin-lesioned (C, D) and nonlesioned control rats (A, B). Note that glucose utilization is reduced in the dentate gyrus molecular layer (DG, arrow) of the IgG-saporin-lesioned animal (C) relative to levels in the non-lesioned animal (A). Decreased glucose utilization is also evident in medial cortical regions, but is relatively unaltered in other brain areas. In B and D, ^{3}H-vesamicol binding is markedly reduced in the prefrontal cortex (PreFCX, arrow) following IgG-saporin injections (D, arrowhead), despite sustained binding levels in the striatum, consistent with loss of cholinergic terminals in the cortex. Findings suggest that i.c.v. IgG-saporin injection damages cholinergic neurons, including basal–forebrain–cortex efferents, and results in chronic depression of functional activity in polysynaptic projection targets of this pathway.

measure of cognitive performance compared to glucose utilization are presented for nonlesioned, control rats and 192 IgG-saporin i.c.v.-injected rats in Table 4.

There was no evidence of a significant dependence between performance in the spatial probe task trial and glucose use in any single region of the 24 brain areas examined in control rats (Table 4). However, in lesioned rats, the degree of correlation with glucose utilization and performance markedly increased in many brain regions, reaching statistical significance in frontal cortex layers IV, V, and VI, DBB, rostral septum, dorsomedial striatum, and the substantia nigra (Table 4).

DISCUSSION

The aim of this study was to gain insight into the inter-dependencies existing between cholinergic deafferentation, cognitive dysfunction and cerebral metabolic impairment in a rodent model. We investigated cholinergic loss, cognitive performance in a maze-learning task, and cerebral metabolism in rats with basal forebrain (BF) cholinergic deficits produced by prior i.c.v. injections of 192-IgG saporin. We have previously shown that cholinergic denervation alters APP processing in the neocortex and hippocampus, which can be modified by muscarinic M1 receptor agonist activation (45, 46). In summary, our results show that a selective depletion of BF cholinerigic neurons results in sustained impairment of glucose utilization in cholinoceptive regions, which is correlated with spatial learning deficits. These findings provide firstly, novel evidence of the long-term selective hypometabolic sequelae of cholinergic denervation, in addition to insights into possible links between cholinergic degener-

TABLE 3

Specific [^{3}H]-Vesamicol Binding in Basal Forebrain Lesioned Rats

Region	Nonlesioned	Saporin-lesioned
BF Cholinergic Projection Targets:		
Prefrontal cortex I–III	0.28 ± 0.04	0.13 ± 0.03*
Prefrontal cortex IV	0.27 ± 0.04	0.10 ± 0.07
Prefrontal cortex V–VI	0.18 ± 0.05	0.09 ± 0.03
Frontal cortex I–III	0.35 ± 0.06	0.29 ± 0.07
Frontal cortex IV	0.33 ± 0.06	0.40 ± 0.09
Frontal cortex V–VI	0.25 ± 0.08	0.27 ± 0.06
Parietal cortex I–III	0.44 ± 0.07	0.31 ± 0.06
Parietal cortex IV	0.47 ± 0.09	0.38 ± 0.13
Parietal cortex V–VI	0.47 ± 0.11	0.27 ± 0.07
Hippocampus: CA1 (rostral)	0.69 ± 0.13	0.20 ± 0.07*
Hippocampus: CA3 (rostral)	0.81 ± 0.11	0.28 ± 0.05*
Dentate gyrus mol. (caudal)	0.81 ± 0.15	0.23 ± 0.05*
Amygdala	3.56 ± 0.20	3.31 ± 0.85
Cholinergic Regions:		
Nucleus accumbens	1.08 ± 0.12	0.75 ± 0.17
Rostral septum	2.35 ± 0.23	2.47 ± 0.33
Striatum: dorsolateral	2.91 ± 0.19	2.56 ± 0.40
Striatum: dorsomedial	0.63 ± 0.10	0.57 ± 0.11
Striatum: ventromedial	0.67 ± 0.09	0.27 ± 0.05*
Nucleus basalis magnocellularis	0.58 ± 0.19	0.51 ± 0.10
Other Regions:		
Globus pallidus	0.14 ± 0.10	0.16 ± 0.04
Substantia nigra pars reticulata	0.02 ± 0.07	0.13 ± 0.08
Substantia nigra pars compacta	0.12 ± 0.10	0.27 ± 0.06
Cerebellum: grey	0.10 ± 0.01	0.29 ± 0.08

Note. Data are mean ± SEM specific [^{3}H]vesamicol binding, (nmol/mg tissue) 18 weeks after i.c.v. injection of 192 IgG-saporin (saporin-lesioned), and in control (nonlesioned) animals (n = 6 per group). Roman numerals indicate layers of cerebral cortex. *P < 0.05, significantly reduced[^{3}H]vesamicol binding, relative to control levels (Student's unpaired t test).

ation, energy metabolic dysfunction and cognitive impairment in AD.

Cholinergic Lesions of the Basal Forebrain by 192 IgG-Saporin

Efferent projections from the nucleus basalis magnocellularis (NBM) region of the BF provide the major extrinsic cholinergic innervation of the neocortex and modulate functional activities including learning, memory and attention, as well as physiological parameters such as cerebral blood flow in the cortex. The NBM also projects to the amygdala (1, 18, 67), while the diagonal band of Broca (DBB) and the medial septum (MS) innervate the hippocampus (16, 65). In the present study, i.c.v. administration of 192 IgG-saporin in rats reduced cholinergic innervation in regions targeted by BF cholinergic projection, notably the prefrontal cortex, hippocampus CA1, CA3, and dentate gyrus, as reflected by lower [^{3}H]-vesamicol binding to presynaptic vesicular ACh transport sites in these regions. Taken with our previous findings of cholinergic neuronal loss in the NBM (with sparing in other regions) and reduced ChAT activity in the hippocampus and cortex following the same 192 IgG-saporin injection paradigm (46), these findings provide further evidence that 192 IgG-saporin i.c.v. injections induce selective cholinergic neuron degeneration in the BF.

Reductions of Cerebral Glucose Metabolism after Cholinergic Deafferentation

We used [^{14}C]-2-deoxyglucose *in vivo* autoradiography to map the effects of cholinergic neuronal and terminal loss on cerebral functional activity, as re-

TABLE 4

Correlations between Local Cerebral Glucose Use and Percentage Time Spent in Target Quadrant on Day 5 in the Water Maze

Region	Nonlesioned (r)	Saporin-lesioned (r)
NBM/Septum cholinergic target regions		
Prefrontal cortex I–III	0.03	0.76
Prefrontal cortex IV	0.03	0.74
Prefrontal cortex V–VI	0.03	0.78
Frontal cortex I–III	0.09	0.74
Frontal cortex IV	0.14	0.81*
Frontal cortex V–VI	0.07	0.90*
Parietal cortex I–III	0.23	0.57
Parietal cortex IV	0.12	0.56
Parietal cortex V–VI	0.26	0.66
Hippocampus: CA1 (rostral)	0.45	0.78
Hippocampus: CA3 (rostral)	0.45	0.74
Dentate gyrus mol. (caudal)	0.28	0.81
Amygdala	0.27	0.71
Cholinergic neuron containing nuclei		
Nucleus accumbens	0.09	0.61
Rostral septum	0.10	0.83*
Striatum: dorsolateral	0.09	0.79
Striatum: dorsomedial	0.01	0.82*
Striatum: ventromedial	0.98	0.68
Nucleus basalis magnocellularis	0.13	0.75
Diagonal band of broca (DBB)	0.09	0.87*
Medial septum	0.64	0.84
Other Regions		
Globus pallidus	0.18	0.59
Substantia nigra pars reticulata	0.11	0.95*
Substantia nigra pars compacta	0.48	0.90*
Cerebellum: grey	0.25	0.73

Note. Data are regression coefficients (r) for each of the 24 cerebral regions investigated, comparing individual animals' performances of percentage of time spent in the target quadrant in a spatial probe task with their respective regional cerebral glucose use values, in 192 IgG-saporin-injected (lesioned) rats. Roman numerals indicate layers of cerebral cortex (n = 6 per group). *P < 0.05, significant correlations (linear regression with the correction of pairwise correlation's).

flected by regional glucose utilization. We demonstrate that reductions in glucose metabolism in cortical and hippocampal regions are still evident 18 weeks postlesion using this cholinergic-selective lesion paradigm. While these reductions were statistically significant in four regions at this time-point (hippocampus CA1, CA3, dentate gyrus molecular layer, and parietal cortex layers V–VI, $P < 0.05$), the consistent trend toward reduced glucose use in all pre-frontal, frontal and parietal cortex regions examined, and in the amygdala (−14–21%), is of added interest. These anatomical subregions correspond to primary NBM cholinergic axonal target zones (35).

Under normal conditions, dynamic changes in glucose utilization predominantly reflect alterations in energy-consuming events in neuron terminals (39). The primary glucose use decreases we report are consistent with chronic down-regulation of terminal activity in cholinergic projection zones, putatively due to reduced or impaired neuronal activation. This fact is highlighted by the close correlations between the relatively large reductions in both glucose utilization rates and specific [^{3}H]-vesamicol binding densities (localizing vesicular Ach transporters, and consequently intact cholinergic neuron terminals) evident in BF cholinergic projection target regions (see Tables 1 and 2). In contrast, other areas selected as control regions (lacking direct cholinergic innervation from the NBM, e.g., cerebellar grey matter, substantia nigra pars reticulata and compacta, globus pallidus) showed little or no reductions in glucose use in 192-saporin-lesioned rats, compared to levels in nonlesioned control animals. However, glucose use changes induced by neuronal degeneration will also impact on secondary and tertiary projection targets of the denervated region. The magnitude of glucose use changes observed in these "down-stream" constituents of polysynaptic functional pathways might be expected to dissipate sequentially along its components, as the relative contributions of neuronal populations unaffected by the primary insult to the overall regional glucose use rate measured, sequentially increase. This may explain the small magnitude, but nonstatistically significant decreases in glucose use evident in regions that are not innervated directly by BF cholinergic efferents. For example, slight hypometabolism in the striatum may reflect the effects of cholinergic denervation of cortical afferent zones, while striatal hypometabolism may impact functional activity in the substantia nigra via striatofugal projections. In addition, the fact that glucose uptake measurements reflect primarily neuron terminal processes does not rule out the possibility of glucose use changes at the site of insult, in this case the BF nuclei, in response to loss of cell bodies in this region. This is supported by a previous study that showed marked hypermetabolism in the NBM region acutely following excitotoxic injection to this region (9). In the present study, measurements were made 18 weeks after selective cholinergic cell death, thus the partial reduction in glucose utilization in the NBM likely reflects some loss of cell bodies with concomitant reduced synaptic activity. Hence glucose use changes seen 18 weeks postcholinergic neuronal loss reflect alterations in well organized, functional pathways associated with the basal forebrain cholinergic system.

Several previous studies in both rats and baboons used different lesion paradigms to assess glucose utilization after disrupting BF cholinergic projections (9, 37, 44, 47, 60, 61, 80). However, these investigations were compromised by the lack of a discrete, selective cholinotoxin. Approaches included electrolytic destruction of NBM neurons, excitotoxin injection directly into the NBM region, and BF injections of the cholinotoxin AF64A. The methodological limitations arise because BF cholinergic neurons are widely dispersed among noncholinergic populations. The utility of AF64A is restricted by dose and injection site parameters (30, 71), while electrolytic techniques lesion not only cell bodies within the target site, but also axons passing through the area. Surgical and excitotoxic lesions of the BF are not sufficiently neuron-specific to produce discrete cholinergic neuronal loss, although recent studies (9, 62, 63) demonstrated that AMPA has greater cholinergic neuron selectivity than other excitotoxins. Furthermore, after unilateral lesioning paradigms, functional recovery may occur due to the influence of the intact contralateral hemispheres.

Previous lesion studies using these approaches reported biphasic effects on cortical glucose utilization. Typically, glucose use was depressed 3–4 days postexcitotoxin-lesion, but recovered to basal levels within 4 weeks after unilateral lesions, and 4 months following bilateral lesions despite sustained ChAT deficits (9, 37, 44, 47, 60, 61, 80). This functional recovery most likely reflects the lack of cholinergic selectivity of these lesion paradigms, leading to incomplete cholinergic denervation. Of these lesion paradigms, AMPA intra-NBM infection appears to be most potent (9). Browne *et al.* (9) showed that ipsilateral cortical glucose use depression was sustained up to 24 days after unilateral AMPA injections into the NBM region. In contrast, as shown by our present studies, i.c.v. injections of 192 IgG-saporin directed against the low affinity NGF receptor (p75NGFR) selectively destroy neurons expressing this receptor, principally cholinergic basal forebrain neurons, without concomitant regional tissue or mechanical damage (29, 71). Furthermore, we demonstrate that both behavioral and cerebral metabolic dysfunction following 192 IgG-saporin injections are still evident 18 weeks postlesion, suggesting that, using this experimental paradigm, the selective cholinergic loss is sufficient to produce sustained metabolic and cognitive deficits more reminicient of the chronic hypometabolism and dementia occurring in AD. This novel obser-

vation of a persistent, long-term decrease in glucose use (and therefore in neuronal functional activity) following 192 IgG-saporin i.c.v. injections, differs from the two previous reports of cerebral metabolism measures following cholinotoxic lesioning with 192 IgG-saporin (3, 52). This reflects the fact that our study employed a bilateral i.c.v. injection paradigm, whereas the previous studies used unilateral lesioning procedures, via unilateral i.c.v. injection (52) or stereotactic NBM lesion (thus only lesioning NBM efferents and sparing hippocampal regions (3)). These studies report a transient increase in glucose use in affected cholinergic projection zones immediately after 192-IgG-saporin injections, which transposed to reduced hippocampal glucose use 30 days after lesion in the i.c.v. injection paradigm (52). Further, neither study investigated effects on glucose use more than 30 days postlesion. Transient patterns of hypometabolism, as seen following many BF lesion approaches, are not typical of AD. PET studies show that metabolic impairments develop during the early stages of AD, most notably in posterior association (parietotemporal and lateral temporal) and prefrontal cortices. Mild hypometabolism in the parietal association cortex of presymptomatic mutation carriers at risk for familial AD has also been reported (22, 31, 36). These glucose use deficits in AD patients, which may reflect both local neuronal degeneration and/or synaptic dysfunction due to cholinergic deafferentation, do not recover over time. Therefore, the observation that 192 IgG-saporin lesions induce long lasting glucose use depression in BF projection targets suggest that this lesion technique may be useful in future to assess the efficacies of potential cholinergic therapeutic approaches.

The Cholinergic System and Cognition

Many animal studies have shown that acetylcholine neurotransmission in both neo- and allocortex can, if disrupted, create severe deficits in cognitive function (20, 21). Deficits in memory tasks have been found after loss of cholinergic input to the hippocampus, based on extensive studies of fimbria-fornix lesions (also creating some extracholinergic damage) (38, 48, 54, 59) or cholinergic degeneration associated with aging (21, 25, 76). NBM lesions, causing loss of neocortical cholinergic input, have suggested an important role for acetylcholine in cortical neurotransmission for attention to stimuli, and therefore indirectly to learning and memory formation (18, 68, 77). During aging, a variety of cellular degenerations are associated with cognitive decline and memory dysfunction. This loss of function has been hypothesized to depend, at least in part, on the decline in acetylcholine levels and cholinergic neuronal systems (2, 12, 14, 66, 72). Cholinergic degeneration is considered to be an important factor underlying memory deficits in neurological disease, such as dementia of Alzheimer's type, and even some Parkinson patients (10, 72, 74, 79). Severity of dementia, number of plaques and, to some degree, loss of synapses, correlate with the degeneration of the cholinergic system in many Alzheimer's patients (27, 65). The precise relationship of the septohippocampal cholinergic system to memory function and symptoms caused by cholinergic neuronal degeneration can be investigated if the model has selective neuronal and terminal loss.

We and others have used the immunotoxic (antibody against NGFr conjugated to saporin) cholinergic lesion model in rodents to assess effects on spatial memory tasks and retention of passive avoidance behavior. After 192-IgG-saporin induced selective cholinergic cell loss in the septo-hippocampal cholinergic system, rats show deficits in acquisition and spatial probe tasks in the Morris swim-maze as well as decreased retention in passive avoidance tests (41, 42). The immunotoxic rodent model of selective degeneration in the septohippocampal cholinergic system thus supports the role of this system in memory-related functions.

The correlations we have observed in the current study of spatial memory (percent time spent in target quadrant on day 5) with brain glucose metabolism are important for in depth functional analysis. First, because the sustained decrease in cerebral glucose utilization is clearly dependent upon the selective loss of cholinergic input, as demonstrated by our lesion method. Moreover, the fact that performance involving spatial components correlated only in lesioned rats with glucose use in frontal cortex and cholinergic neuron containing nuclei may indicate that the lesioned brain is more dependent and has less distributed function of brain areas during performance of such tasks compared to intact and normal rats (see Table 4). This functional analysis suggests that even though the saporin-lesioned rats are defective in their cognitive performance, they are still attempting to solve the task through routes that have previously been demonstrated to be important for spatial memory processing. Some of the behavioral correlations, such as with local cerebral metabolism in the dorsomedial striatum and substantia nigra may not be easily understood from simple anatomical single circuit diagrams. However, much of this spatial and mnemonic processing obviously is going through a number of dependent circuitries and certainly striatum is an important component in subcortical processing, also for cognition (see 17, 33, 78), and could therefore have some relevance to the overall performance *of the lesioned rats*. The increased correlation to performance with substantia nigra in the lesioned rats is harder to interpret, but stands as a possible downstream effector region for the many consequences of impaired performance, such as is seen in locomotor hyperactivity of rats with cholinergic deficits or after atropine treatment, and may therefore be ex-

plained as a hyperactivity syndrome. Such deficits may also play a role in passive avoidance and in swim maze tests (43). Nonetheless, the important relative decrease in local glucose utilization and its correlations with specific behavior may be important in understanding of cognitive processing with dysfunctional cholinergic components of the corticohippocampal system.

Cerebral Metabolic Function and APP Processing

Several lines of evidence demonstrate the existence of metabolic defects and increased oxidative stress in AD. Impaired glucose uptake in brain regions exhibiting neuritic plaques occurs in AD patients (34), and deficits in cerebral glucose utilization may occur early in the process of the disease, preceding neuronal degeneration (36). Decreased activity of mitochondrial metabolic enzymes, including dehydrogenases and cytochrome c oxidase has been reported in AD brain (6), while glucose uptake transporters are also down-regulated (73). Of importance, recent evidence suggests a mechanistic link between disturbed energy metabolism and altered APP processing. Inhibiting mitochondrial energy metabolism with sodium azide leads to markedly enhanced amyloidogenic processing of APP in cell lines (24). Furthermore, Gasparini *et al.* (26) reported that both glucose deprivation and inhibiting energy metabolism with sodium azide reduced APPs secretion, while treatment with the antioxidant glutathione fully reversed azide's inhibitory effect. Hypoglycemia elevates the expression of APP mRNA in astroglial cells, and leads to enhanced alternative APP splicing that encodes a kunitz-type serine protease inhibitor domain, which has been shown to partially counteract the Aβ degradation (55). Also, Copani *et al.* (13) observed enhanced Aβ toxicity in mouse cortical neuronal culture following energy failure after glucose deprivation. APPs is postulated to be protective against excitotoxic, metabolic, and oxidative insults (51), and thus reduced levels of APPs due to metabolic dysfunction may be detrimental to neurons. Taken with our previous finding of elevated APP levels in the animal model used in this study (45, 46), these observations suggests that impaired energy metabolism may contribute to the pathogenesis of AD by altering APP processing, leading to reduced APP secretion and increased amyloidogenic derivatives. As a consequence, altered APP processing may in turn disrupt energy metabolic function further. Interestingly, this hypothesis is further supported by findings that transgenic mice overexpressing human APP exhibit reductions in cerebral glucose metabolism (32). In addition, human APP expression in hippocampal and cortical neurons impairs glucose transport and suppresses ATP production by a mechanism involving membrane lipid peroxidation (49). Overall, the results reported in this study strengthen the argument that APP processing and energy metabolism in the brain are functionally related, and modulation of APP processing resulting from impaired energy metabolism could play a significant role in the pathogenesis of AD.

ACKNOWLEDGMENTS

This work was supported in part by a donation from the Irving and Betty Brudnick Research Fund at McLean Hospital. We also acknowledge Ms. Stephanie Berger for technical assistance in the *in vivo* autoradiographic studies.

REFERENCES

1. Barbelivien, A., E. T. MacKenzie, and F. Dauphin. 1995. Regional cerebral blood flow responses to neurochemical stimulation of the substantia innominata in the anaesthetized rat. *Neurosci. Lett.* **190:** 81–84.
2. Bartus, R., R. L. Dean, C. Beer, and A. S. Lippa. 1982. The cholinergic hypothesis of geriatric memory dysfunction. *Science* **217:** 408–417.
3. Bassant, M. H., F. Poindessous-Jazat, and B. H. Schmidt. 2000. Sustained effect of metrifonate on cerebral glucose metabolism after immunolesion of basal forebrain cholinergic neurons in rats. *Eur. J. Pharmacol.* **387:** 151–162.
4. Behl, C., J. Davis, G. M. Cole, and D. Schubert. 1992. Vitamin E protects nerve cells from amyloid beta protein. *Biochem. Biophys. Res. Commun.* **186:** 944–950.
5. Behl, C., J. B. Davis, R. Lesley, and D. Schubert. 1994. Hydrogen peroxide mediates amyloid beta protein toxicity. *Cell* **77:** 817–827.
6. Blass, J. 1993. Metabolic alterations common to neural and nonneural cells in Alzheimer's disease. *Hippocampus* **3:** 45–54.
7. Bowen, D. M., J. S. Benton, J. A. Spillane, C. C. Smith, and S. J. Allen. 1982. Choline acetyltransferase activity and histopathology of frontal neocortex from biopsies of demented patients. *J. Neurol. Sci.* **57:** 191–202.
8. Bowen, D. M., C. B. Smith, P. White, and A. N. Davison. 1976. Neurotransmitter-related enzymes and indices of hypoxia in senile dementia and other abiotrophies. *Brain* **99:** 459–496.
9. Browne, S. E., J. Muir, T. W. Robbins, K. J. Page, B. J. Everitt, and J. McCulloch. 1998. The cerebral metabolic effects of manipulating glutamatergic systems within the basal forebrain in conscious rats. *Eur. J. Neurosci.* **10:** 649–663.
10. Candy, J. M., R. H. Perry, E. K. Perry, D. Irving, G. Blessed, A. F. Fairbairn, and B. E. Tomlinson. 1983. Pathological changes in the nucleus of Meynert in Alzheimer's and Parkinson's diseases. *J. Neurol. Sci.* **59:** 277–289.
11. Chalmers, D. T., and J. McCulloch. 1991. Alterations in neurotransmitter receptors and glucose use after unilateral orbital enucleation. *Brain Res.* **540:** 243–254.
12. Cohen, B. M., P. F. Renshaw, A. L. Stoll, R. J. Wurtman, D. Yurgelun-Todd, and S. M. Babb. 1995. Decreased brain choline uptake in older adults. An in vivo proton magnetic resonance spectroscopy study. *J. Am. Med. Assoc.* **274:** 902–907.
13. Copani, A., J.-Y. Koh, and C. Cotman. 1991. β-Amyloid increases neuronal susceptibility to injury by glucose deprivation. *Neuroreport* **2:** 763–765.

14. Coyle, J. T., D. L. Price, and M. R. DeLong. 1983. Alzheimer's disease: A disorder of cortical cholinergic innervation. *Science* **219:** 1184–1190.

15. Custers, F. G., J. E. Leysen, J. C. Stoof, and J. D. Herscheid. 1997. Vesamicol and some of its derivatives: Questionable ligands for selectively labelling acetylcholine transporters in rat brain. *Eur. J. Pharmacol.* **338:** 177–183.

16. Davies, P., and A. J. F. Maloney. 1976. Selective loss of central cholinergic neurons in Alzheimer's disease. *Lancet* **2:** 1403–1404.

17. Divac, I., H. J. Markowitsch, and M. Pritzel. 1978. Behavioral and anatomical consequences of small intrastriatal injections of kainic acid in the rat. *Brain Res.* **151:** 523–532.

18. Dunnett, S., B. Everitt, and T. Robbins. 1991. The basal forebrain cortical cholinergic system: Interpreting the functional consequences of excitotoxic lesions. *Trends Neurosci.* **14:** 494–501.

19. Durara, R., C. Grady, J. Haxby, M. Sundaram, N. R. Cutler, L. Heston, A. Moore, N. Schlageter, S. Larson, and S. I. Rapoport. 1986. Position emission tomography in Alzheimer's disease. *Neurology* **36:** 879–887.

20. Fibiger, H. C. 1991. Cholinergic mechanisms in learning, memory and dementia: A review of recent evidence. *Trends Neurosci.* **14:** 220–223.

21. Fischer, W., F. H. Gage, and A. Bjorklund. 1989. Degenerative changes in forebrain cholinergic nuclei correlate with cognitive impairments in aged rats. *Eur. J. Neurosci.* **1:** 33–45.

22. Frackowiak, R. S., C. Pozzilli, N. J. Legg, G. H. DuBoulay, J. Marshall, G. L. Lenzi, and T. Jones. 1981. Regional cerebral oxygen supply and utilization in dementia: A clinical and physiological study with oxygen-15 and position tomography. *Brain* **104:** 753–778.

23. Fukuyama, H., K. Harada, H. Yamaguchi, T. Miyoshi, S. Yamaguchi, J. Kimura, M. Kameyama, M. Senda, Y. Yonekura, and J. Konishi. 1991. Coronal reconstruction images of glucose metabolism in Alzheimer's disease. *J. Neurol. Sci.* **106:** 128–134.

24. Gabuzda, D., J. Busciglio, L. Chen, P. Matsudaira, and B. Yankner. 1994. Inhibition of energy metabolism alter the processing of amyloid precursor protein and induces a potentially amyloidogenic derivative. *J. Biol. Chem.* **269:** 13623–13628.

25. Gage, F. H., A. Björklund, U. Stenevi, S. B. Dunnett, and P. A. T. Kelly. 1984. Intrahippocampal septal grafts ameliorate learning impairments in aged rats. *Science* **225:** 533–536.

26. Gasparini, L., M. Racchi, L. Benussi, D. Curti, G. Binetti, A. Bianchetti, M. Trabucchi, and S. Govoni. 1997. Effect of energy shortage and oxidative stree on amyloid precursor protein metabolism in COS cells. *Neurosci. Lett.* **231:** 113–117.

27. German, D. C., C. L. White, and D. R. Sparkman. 1987. Alzheimer's disease: Neurofibrally tangles in nuclei that project to the cerebral cortex. *Neuroscience* **21:** 305–312.

28. Goodman, Y., and M. Mattson. 1994. Secreted forms of β-amyloid precursor protein protect hippocampal neurons against amyloid β-peptide-indused oxidative injury. *Exp. Neurol.* **128:** 1–12.

29. Gutierrez, H., R. Gutierrez, R. Silva-Gandarias, J. Estrada, M. I. Miranda, and F. Bermuderez-Rattoni. 1999. Differential effects of 192IgG-saporin and NMDA-induced lesions into the basal forebrain on cholinergic activity and taste aversion memory formation. *Brain Res.* **834:** 136–141.

30. Hanin, I. 1996. The AF64A model of cholinergic hypofunction: An update. *Life Sci.* **58:** 1955–1964.

31. Haxby, J. V. 1990. Cognitive deficits and local metabolic changes in dementia of the Alzheimer's type. In *Imaging, Cerebral Topography and Alzheimer's Disease* (S. R. Rapoport, H. Petit, D. Leys, and Y. Christen, Eds.), pp. 109–119. Springer-Verlag, Berlin.

32. Hsiao, K. K., D. R. Borchelt, K. Olson, R. Johannsdottir, C. Kitt, W. Yunis, S. Xu, C. Eckman, S. Younki, D. Price, C. Ladecola, H. B. Clark, and G. Carlson. 1995. Aged-related CNS disorder and early death in transgenic FVB/N overexpressing Alzheimer amyloid precursor protein. *Neuron* **15:** 1203–1218.

33. Isacson, O., S. B. Dunnett, and A. Bjorklund. 1986. Behavioural recovery in an animal model of Huntington's disease. *Proc. Natl. Acad. Sci. USA* **83:** 2728–2732.

34. Jagust, W. J., J. P. Seab, R. H. Huesman, P. E. Valk, C. A. Mathis, B. R. Reed, P. G. Coxson, and T. F. Budinger. 1991. Diminished glucose transport in Alzheimer's disease: Dynamic PET studies. *J. Cereb. Blood Flow Metab.* **11:** 323–330.

35. Johnston, M., M. McKinney, and J. T. Coyle. 1981. Neocortical cholinergic innervation: A description of extrinsic and intrinsic components in the rat. *Exp. Brain Res.* **43:** 159–172.

36. Kennedy, A., R. Frackowiak, S. Newman, P. Bloomfield, J. Seaward, P. Roques, G. Lewington, V. Cunningham, and M. Rossor. 1995. Deficits in cerebral glucose metabolism demonstrated by position emmission tomography in individuals at risk of familial Alzheimer's disease. *Neurosci. Lett.* **186:** 17–20.

37. Kiyosawa, M., J.-C. Baron, E. Hamel, S. Papata, D. Duverger, D. Riche, B. Mazoyer, R. Naquet, and E. Mackenzie. 1989. Time course of effects of unilateral lesions of the nucleus basalis of Meynert on glucose utilization by the cerebral cortex. *Brain* **112:** 435–455.

38. Kordower, J. H., and M. S. Fiandaca. 1990. Response of the monkeys cholinergic septohippocampal system to fornix transection: A histochemical and cytochemical analysis. *J. Comp. Neurol.* **298:** 443–457.

39. Kurumaji, A., D. Dewar, and J. McCulloch. 1993. Metabolic mapping with deoxyglucose autoradiography as an approach for assessing drug action in the central nervous system. In *Imaging Drug Action in the Brain* (E. London. Eds.), pp. 207–246. CRC Press.

40. Leanza, G. 1998. Chronic elevation of amyloid precursor protein expression in the neocortex and hippocapmus of rats with selective cholinergic lesions. *Neurosci. Lett.* **257:** 53–56.

41. Leanza, G., O. G. Nilsson, R. G. Wiley, and A. Björklund. 1995. Selective lesioning of the basal forebrain cholinergic system by intraventricular 192 IgG-saporin: Behavioural, biochemical and stereological studies in the rat. *Eur. J. Neurosci.* **7:** 329–343.

42. LeBlanc, C., L. Burns, P. Borghesani, T. Deacon, J. Dinsmore, and O. Isacson. 1996. Xenotransplanted cholinergic neurons into animal models of cognitive dysfunction. *Soc. Neurosci.* **22:** 578. [Abstract]

43. LeBlanc, C. J., T. W. Deacon, B. R. Whatley, J. Dinsmore, L. Lin, and O. Isacson. 1999. Morris water maze analysis of 192-IgG-saporin lesioned rats and porcine cholinergic transplants to the hippocampus. *Cell Trans* **8:** 131–143.

44. LeMestric, C., C. Chavoix, F. Chapon, F. Mezenge, J. Epelbaum, and J. C. Baron.1998. Effects of damage to the basal forebrain on brain glucose utilization: A reevaluation using positron emission tomography in baboons with extensive unilateral excitotoxic lesion. *J. Cereb. Blood Flow Metab.* **18:** 476–490.

45. Lin, L., B. Georgievska, A. Mattsson, and O. Isacson. 1999. Cognitive changes and modified processing of amyloid precur-

sor protein in the cortical and hippocampal system after cholinergic synapse loss and muscarinic receptor activation. *Proc. Natl. Acad. Sci. USA* **96:** 12108–12113.

46. Lin, L., C. Leblanc, T. Deacon, and O. Isacson. 1998. Chronic cognitive decifits and amyloid precursor protein elevation after immunotoxin lesions of the basal forebrain cholinergic system. *Neuroreport* **9:** 547–52.
47. London, E., M. McKinney, M. Dam, A. Ellis, and J. T. Coyle. 1984. Decreased cortical glucose utilization after ibotenate lesions of the rat ventromedial globus pallidus. *J. Cereb. Blood Flow Metab.* **4:** 381–390.
48. Mahut, H. 1972. A selective spatial deficit in monkeys after transection of the fornix. *Neuropsychologia* **10:** 65–74.
49. Mark, R., Z. Pang, J. Geddes, K. Uchida, and M. Mattson. 1997. Amyloid β-peptide impairs glucose transport in hippocampal and cortical neurons: Involvement of membrane lipid peroxidation. *J. Neurosci.* **17:** 1046–1054.
50. Mattson, M., S. Barger, B. Cheng, I. Lieberburg, V. Smith-Swintosky, and R. Rydel. 1993. beta-amyloid precursor protein metabolites and loss of neuronal Ca2+ homeostasis in Alzheimer's disease. *Trends Neurosci.* **16:** 409–414.
51. Mattson, M. P., and W. A. Pedersen. 1998. Effects of amyloid precursor protein derivatives and oxidative stress on basal forebrain cholinergic systems in Alzheimer's disease. *Int. J. Dev. Neurosci.* **16:** 737–753.
52. Mehlhorn, G., T. Loffler, J. Apelt, S. Rossner, T. Urabe, N. Hattori, S. Nagamatsu, V. Bigl, and R. Schliebs. 1998. Glucose metabolism in cholinoceptive cortical rat brain regions after basal forebrain cholinergic lesion. *Int. J. Dev. Neurosci.* **16:** 675–90.
53. Muller, D. M., K. Mendla, S. A. Farber, and R. M. Nitsch. 1997. Muscarinic M1 receptor agonists increase the secretion of the amyloid precursor protein ectodomain. *Life Sci.* **60:** 985–998.
54. Murray, E. A., M. Davidson, D. Gaffan, D. S. Olton, and S. Suomi. 1989. Effects of fornix transection and cingulate cortical ablation on spatial memory in rhesus monkeys. *Exp. Brain Res.* **74:** 173–186.
55. Naidu, A., B. Quon, and B. Cordell. 1995. β-Amyloid peptide produced *in vitro* is degraded by proteinases released by culture cells. *J. Biol. Chem.* **270:** 1369–1374.
56. Nitsch, R. M. 1996. From acetylcholine to Amyloid: Neurotransmitters and the pathology of Alzheimer's disease. *Neurodegeneration* **5:** 477–482.
57. Nitsch, R. M., M. Deng, M. Tennis, D. Schoenfeld, and J. H. Growdon. 2000. The selective muscarinic M1 agonist AF102B decreases levels of total Aβ in cerebrospinal fluid of patients with Alzheimer's disease. *Ann. Neurol.* **48:** 913–918.
58. Nitsch, R. M., S. A. Farber, J. H. Growdon, and R. J. Wurtman. 1993. Release of amyloid β-protein precursor derivatives by electrical depolarization of rat hippocamal slices. *Proc. Natl. Acad. Sci. USA* **90:** 5191–5193.
59. Olton, D. S., J. T. Becker, and G. E. Handelmann. 1979. Hippocampus, space and memory. *Behav. Brain Sci.* **2:** 313–365.
60. Orzi, F., G. Diana, F. Casamenti, E. Palombo, and C. Fieschi. 1988. Local cerebral glucose utilization following unilateral and bilateral lesions of the nucleus basalis magnocellularis in the rat. *Brain Res.* **462:** 99–103.
61. Ouchi, Y., H. Fukuyama, M. Ogawa, H. Yamauchi, J. Kimura, Y. Magata, Y. Yonekura, and J. Konishi. 1996. Cholinergic projection from the basal forebrain and cerebral glucose metabolism in rats: a dynamic PET study. *J. Cereb. Blood Flow Metab.* **16:** 34–41.
62. Page, K., B. J. Everitt, T. W. Robbins, H. M. Marston, L. S. Wilkinson. 1991. Dissociable effects on spatial maze and passive avoidance acquisition and retention following AMPA and ibotenic acid-induced excitotoxic lesions of the basal forebrain in rats: Differential dependence on cholinergic neuronal loss. *Neuroscience* **43:** 457–472.
63. Page, K., D. J. S. Sirinathsinghji, and B. J. Everitt. 1995. AMPA-induced lesions of the basal forebrain differentially affect cholinergic and non-cholinergic neurons: Lesion assessment using quantitative *in situ* hybridization histochemistry. *Eur. J. Neurosci.* **7:** 1012–1021.
64. Paxinos, G., and C. Watson. 1986. *The Rat Brain in Stereotaxic Coordinates*, 2nd ed. Academic Press.
65. Perry, E., B. Tomlinson, G. Blessed, K. Bergmann, P. Gibson, and R. Perry. 1978. Correlation of cholinergic abnormalities with senile plaques and mental test scores in senile dementia. *Br. Med. J.* **2:** 1457–1459.
66. Perry, E. K., R. H. Perry, G. Blessed, and B. D. Tomlinson. 1977. Necropsy evidence of central cholinergic deficits in senile dementia. *Lancet* **1:** 189.
67. Richardson, R., and M. R. Delong. 1988. A reappraisal of the functions of the nucleus basalis of Meynert. *Trends Neurosci.* **11:** 264–267.
68. Richardson, R. T., and M. R. Delong. 1991. Functional aspects of the basal forebrain cholinergic system. In *Activation to Acquisition* (R. T. Richardson, Eds.), pp. 135–166, Birkhauser, Boston.
69. Rogers, G. A., S. M. Parsons, D. C. Anderson, L. M. Nilsson, B. A. Bahr, W. D. Kornreich, R. Kaufman, R. S. Jacobs, and B. Kirtman. 1989. Synthesis, in vitro acetylcholine-storage-blocking activities, and biological properties of derivatives and analogues of trans-2-(4-phenylpiperidino) cyclohexanol (vesamicol). *J. Med. Chem.* **32:** 1217–30.
70. Rossner, S., U. Ueberham, J. Yu, L. Kirazov, S. Reinhard, J. R. Perez-Polo, and V. Bigl. 1997. In vivo regulation of amyloid precursor protein secretion in rat neocortex by cholinergic activity. *Eur. J. Neurosci.* **9:** 2125–2134.
71. Schliebs, R., S. Rossner, and V. Bigl. 1996. Immunolesion by 192IgG-saporin of rat basal forebrain cholinergic system: A useful tool to produce cortical cholinergic dysfunction. *Prog. Brain Res.* **109:** 253–264.
72. Scinto, L. F., K. R. Daffner, D. Dressler, B. I. Ransil, D. Rentz, S. Weintraub, M. Mesulam, and H. Potter. 1994. A potential noninvasive neurobiological test for Alzheimer's disease. *Science* **266:** 1051–1054.
73. Simpson, I. A., K. R. Chundu, T. Davies-Hill, W. G. Honer, and P. Davies. 1994. Decreased concentrations of GLUT1 and GLUT3 glucose transporters in the brains of patients with Alzheimer's disease. *Ann. Neurol.* **35:** 546–551.
74. Sims, N. R., D. M. Bowen, S. J. Allen, C. C. T. Smith, T. Neary, D. J. Thomas, and A. N. Davison. 1983. Presynaptic cholinergic dysfunction in patients with dementia. *J. Neurochem.* **40:** 503–509.
75. Sokoloff, L., M. Reivich, C. Kennedy, M. H. Des Rosiers, C. S. Patlak, K. D. Pettigrew, O. Sakurada, and M. Shinohara. 1977. The [$_{14}$C]2-deoxyglucose method for the measurement of local cerebral glucose utilization. Theory, procedure, and normal values in the conscious and anaesthetized rat. *J. Neurochem.* **28:** 897–916.
76. Stroessner-Johnson, H. M., P. R. Rapp, and D. G. Amaral. 1992. Cholinergic cell loss and hypertrophy in the medial septal nucleus of the behaviorally characterized aged rhesus monkey. *J. Neurosci.* **12:** 1936–1944.

77. Voytko, M. R., D. S. Olton, R. T. Richardson, L. K. Gorman, J. R. Tobin, and D. L. Price. 1994. Basal forebrain lesions in monkeys disrupt attention but not learning and memory. *J. Neurosci.* **14:** 167–186.

78. Whishaw, I. O., G. Mittleman, S. T. Bunch, and S. B. Dunnett. 1987. Impairments in the acquisition, retention and selection of spatial navigation strategies after medial caudate-putamen lesions in rats. *Behav. Brain Res.* **24:** 125–138.

79. Whitehouse, P. J., D. L. Price, A. W. Clark, J. T. Coyle, and M. R. DeLong. 1981. Alzheimer's disease: Evidence for selective loss of cholinergic neurons in the nucleus basalis. *Ann. Neurol.* **10:** 122–126.

80. Yamaguchi, T., M. Kunimoto, S. Pappata, C. Chavoix, E. Brouillet, D. Riche, M. Maziere, R. Naquet, E. T. Mackenzie, and J. C. Baron. 1990. Effects of unilateral lesions of the nucleus basalis of Meynert on glucose utilization in callostomized baboons: A PET study. *J. Cereb. Blood Flow Metab.* **10:** 618–623.

81. Yankner, B. A., L. K. Duffy, and D. A. Kirschner. 1990. Neurotrophic and neurotoxic effects of amyloid β protein: Reversal by tachykinin neuropeptides. *Science* **250:** 279–282.